

Effect of Synthetic Parameters on Synthesis of Magnesium Aluminum Spinels

Jinxia Duan¹, Xiuhui Wang¹, Youfei Zhang¹, Hong Gao¹, Yan Xie^{2*}, Jinlong Yang³

¹School of Materials and Engineering, Dalian Jiaotong University, Dalian, China

²Gold Catalysis Research Center, State Key Laboratory of Catalysis, Dalian Institute of Chemical Physics, Chinese Academy of Sciences, Dalian, China

³State Key Laboratory of New Ceramics and Fine Processing, School of Materials Science and Engineering, Tsinghua University, Beijing, China

Email: *yanxie@dicp.ac.cn

How to cite this paper: Duan, J.X., Wang, X.H., Zhang, Y.F., Gao, H., Xie, Y. and Yang, J.L. (2019) Effect of Synthetic Parameters on Synthesis of Magnesium Aluminum Spinels. *Journal of Materials Science and Chemical Engineering*, 7, 1-15.
<https://doi.org/10.4236/msce.2019.73001>

Received: February 3, 2019

Accepted: March 24, 2019

Published: March 27, 2019

Copyright © 2019 by author(s) and Scientific Research Publishing Inc.

This work is licensed under the Creative Commons Attribution International

License (CC BY 4.0).

<http://creativecommons.org/licenses/by/4.0/>



Open Access

Abstract

In this work, the magnesium aluminum spinel ($MgAl_2O_4$) was prepared by Mg and Al as precursors through a method of sol-gel subsequent with high temperature calcination. The wide range of synthetic conditions, including organic alcohols, ammonia content, dispersant, alkoxide concentration, hydrolysis time, hydrolysis temperature and calcination temperature were screened over as-prepared samples. This work provides a necessary experimental basis for the synthesis of $MgAl_2O_4$ with uniform particle size of spherical structure, which has a potential to be used in many industrial and military applications.

Keywords

Alkoxide Hydrolysis, $MgAl_2O_4$, Synthetic Parameters

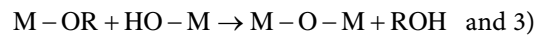
1. Introduction

As one of well-known spinels (typically refers to AB_2O_4 , A^{2+} , B^{3+} or A^{4+} , B^{2+}), magnesium aluminate ($MgAl_2O_4$) has been mainly developed and applied in industrial and military applications, including high-pressure arc lamps, transparent armor, optical heat exchangers, and missile domes [1] [2] [3] [4] [5]. Among them, appropriate transparent ceramic based materials were employed due to its unique properties, like high thermal stability with high melting point of 2135°C [6], unique optical properties and mechanical strength at high temperature. With increasing utilizations of catalyst and support, $MgAl_2O_4$ spinel has been synthesized with high purity, small particle size with uniform pore size

distribution and high surface area. Therefore, it is crucial to widely investigate on the synthetic parameters of MgAl_2O_4 [7]. So far, several approaches were introduced for the preparation of MgAl_2O_4 , namely solid-state [8] [9], sol-gel [10] [11] [12] [13], spray drying [14] and co-precipitation [15] [16]. Especially, sol-gel is considered to be one of the most effective methods focused on the synthesis of MgAl_2O_4 . Any positive ions can be introduced during the hydrolysis process. Besides, the reaction conditions of alkoxide hydrolysis are mild with various advantages, such as simple operation, high purity of product and small particle size, leading to the final high activity. It is known that alkoxide hydrolysis has been extensively used not only on the development of nano-alumina powder but also on the synthesis of MgAl_2O_4 [17] [18]. To the best of our knowledge, few investigations were reported on the synthetic parameters for preparation of MgAl_2O_4 via alkoxide hydrolysis [18]. Great efforts have been made on the features of metal alkoxides, particularly in the preparation of high-purity oxide powders of uniform size, shape as well as the composition.

Herein, discussion on the synthetic parameters on MgAl_2O_4 through alkoxide hydrolysis was introduced by $\text{Mg}[\text{Al}(\text{OR})_4]_2$ derived from Mg, Al and isopropanol by tuning the reaction conditions and synthetic factors. In this work, several synthetic influenced factors (especially refer to type of organic alcohol, pH, aging time, temperature, etc.) were considered on the effect of the structure and size distribution of as-acquired samples.

It has been known that three reactions simultaneously occur based on hydrolysis theory for alkoxide, namely 1) hydrolysis reaction process



$\text{M}-\text{OH} + \text{HO}-\text{M} \rightarrow \text{M}-\text{O}-\text{M} + \text{H}_2\text{O}$. It is believed that the hydrolysis of $\text{MgAl}_2(\text{OC}_3\text{H}_8)_8$ is incomplete with much lower content of water. The hydrolysis rate is boosted at the point of too much water. The hydrolyzed product of $\text{MgAl}_2(\text{OH})_8$ incompletely disperse, resulting in agglomeration and enlargement of the particles. Therefore, moderate of hydrolysis rate is favorable to obtain uniform particle size with well-dispersibility at 40°C for 24 h with CTAB at pH value of 8.5. As a result, the obtained $\text{MgAl}_2(\text{OH})_8$ was further calcined at 1200°C for preparation of MgAl_2O_4 . This study further opens a new avenue to supply an optimal synthetic route to achieve pure metal oxides by hydrolysis, which can be widely applied in the fields of industrial production and military applications.

2. Experimental

2.1. Chemicals

Mg foil (99.9%), Al foil (99.9%) and Anhydrous aluminum chloride (AR) were obtained from Tianjin Bodi Chemical Co., Ltd. Cetyltrimethylammonium bromide (CTAB, AR) and polyvinyl pyrrolidone (PVP) were purchased from Shanghai Reagents Factory. $\text{AlF}_3 \cdot 3.5\text{H}_2\text{O}$ (CP) was got from Shanghai Reagent

Third Factory. Alcohol (AR), isopropanol (AR) and n-butanol (AR) were obtained from Liaodong Chemical Reagent Factory. The deionized water was directly made in the experiment.

2.2. Preparation of MgAl₂O₄

Preparation of alkoxide: Mg and Al foils were first grinded and cleaned with ethanol. The treated Mg and Al were weighed and added into the reaction kettle based on the stoichiometric ratio of MgAl₂O₄ with the addition of trace AlF₃ and excess isopropanol. After heated at 85°C under reflux, the product of MgAl₂(OC₃H₈)₈ was obtained after distillation. Here, in the experiment organic alcohols of ethanol and n-butanol were selected under reflux at corresponding boiling point for comparison.

Alkoxide hydrolysis: Organic alcohol and deionized water were prepared to hydrolysate with a volume ratio of 1:1. NH₃·H₂O (1.5 mL) and CTAB (0.75 mL) were added into 50 mL above hydrolysate stirring under constant temperature water bath. Colorless transparent sol of MgAl₂(OH)₈ was obtained by addition of 10 g MgAl₂(OC₃H₈)₈ with dropwise at a rate of 0.1 mL·min⁻¹ under continuous stirring in the water bath at 40°C for 24 h. In this experiment procedure, several synthesis parameters, like alkoxide addition amount, proportion of isopropanol and deionized water in hydrolysate, hydrolysis temperature and time, pH value, the addition of dispersant (refers to CTAB and PVP) were further investigated keeping other parameters consistent.

Preparation of MgAl₂O₄: The MgAl₂(OH)₈ sol synthesized via alkoxide hydrolysis was further dried at 80°C for 4 h and calcined at 1200°C for 2 h in a box-type resistance furnace. As a result, the sample of magnesium aluminum spinel powder was obtained for further characterization.

2.3. Characterization

The weight loss was tested by TGA (600, USA, TAQ) under N₂ with warming speed of 5°C·min⁻¹. X-ray diffraction (XRD) analysis was recorded on a D/max-3B X-ray diffractometer (CuK α radiation, $\lambda = 1.54056\text{ \AA}$) to detect the structure of samples in a scanning range 2 θ of 5 to 80° with operating voltage at 40 kV and the current of 35 mA with a scanning rate of 2°·min⁻¹. The Brunauer-Emmet-Teller (BET) specific surface area and porous properties were measured through N₂ adsorption-desorption at -196°C on a Quadrasorb SI instrument (Quantachrome, USA). A field-emission scanning electron microscope (SEM) was operated on a JSM-6360LV instrument (JEOL Corporation) to describe the morphology of samples at the accelerating voltage of 5.0 kV. A mater sizer 2000 laser particle size analyzer (Malvern Corporation, UK) was used to measure the particle size and its distribution.

3. Results and Discussion

3.1. Effect on Organic Alcohols

Initially, different organic alcohols, including ethanol, isopropanol and n-butanol

were selected to investigate its effect on the particle size of precursors. The particle size and surface area of corresponding samples are listed in **Figure 1** and **Table 1**. It can be seen that the particle size distribution of powder prepared with ethanol and isopropanol is relatively concentrated compared to that of powders synthesis with n-butanol. The sample with n-butanol possesses twice as much as that at D90 (the cumulative particle size distribution of a sample reaching 90%) relative to other two samples. It might be the reason that partially negatively charged $\text{HO}^{\delta-}$ group nucleophilic attack with a partially positively charged metal atom $\text{M}^{\delta+}$ during the hydrolysis process. Meanwhile, positively charged protons are transferred to a negatively charged $\text{OR}^{\delta-}$. Finally, the protonated protonated $\text{OR}^{\delta+}$ is separated from the metal atom M. The large molecular structure of magnesium n-butoxide results in relatively weak between alkoxy $\text{OR}^{\delta+}$. Metal bond and $\text{OR}^{\delta+}$ rapidly desorbs from the metal atom to form magnesium hydroxide aluminum particles leading to hydrogen hydroxide in a short time. Besides, the particles are easier to agglomerate and consequently the particle size of corresponding powder with n-butanol has a relatively dispersion. With comprehensive analysis of samples with different alcohols, the sample with isopropanol displays a larger surface area with uniform particle size.

3.2. Effect of Ammonia Content

The concentration of ammonia was also taken accounted in the synthesis of hydrolysis magnesium aluminum alkoxide, in which ammonia was used to adjust

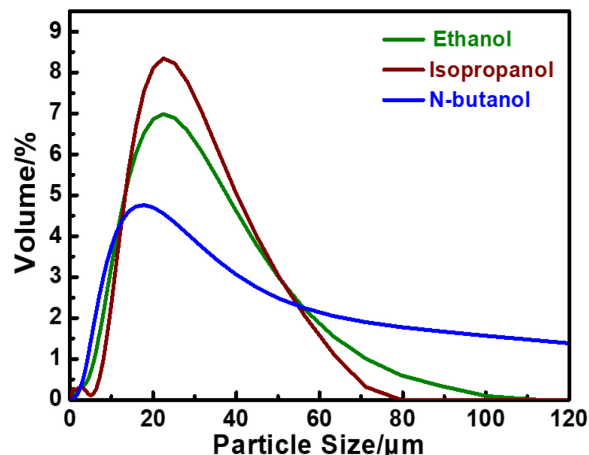


Figure 1. The size distribution of alkoxides with various alcohols of ethanol, isopropanol and n-butanol.

Table 1. The particle size and specific surface area of samples with various alkoxides.

Alkoxides with types of alcohols	D10 (μm)	D50 (μm)	D90 (μm)	Surface area (m^2/g)
Ethanol	7.439	19.719	43.041	5.16
Isopropanol	9.621	20.874	40.475	5.51
N-butanol	6.280	19.932	102.283	4.47

the pH value of the system. **Figure 2** displays the ammonia concentration effect on the particle size and size distribution of powders hydrolysis at 20°C for 2 h. Obviously, the average particle size gradually increases with the increasing ammonia content from 0.5 to 3.0 mL. The well-dispersion of powder with 0.5 mL ammonia content can be acquired by scanning electron microscope (SEM) in

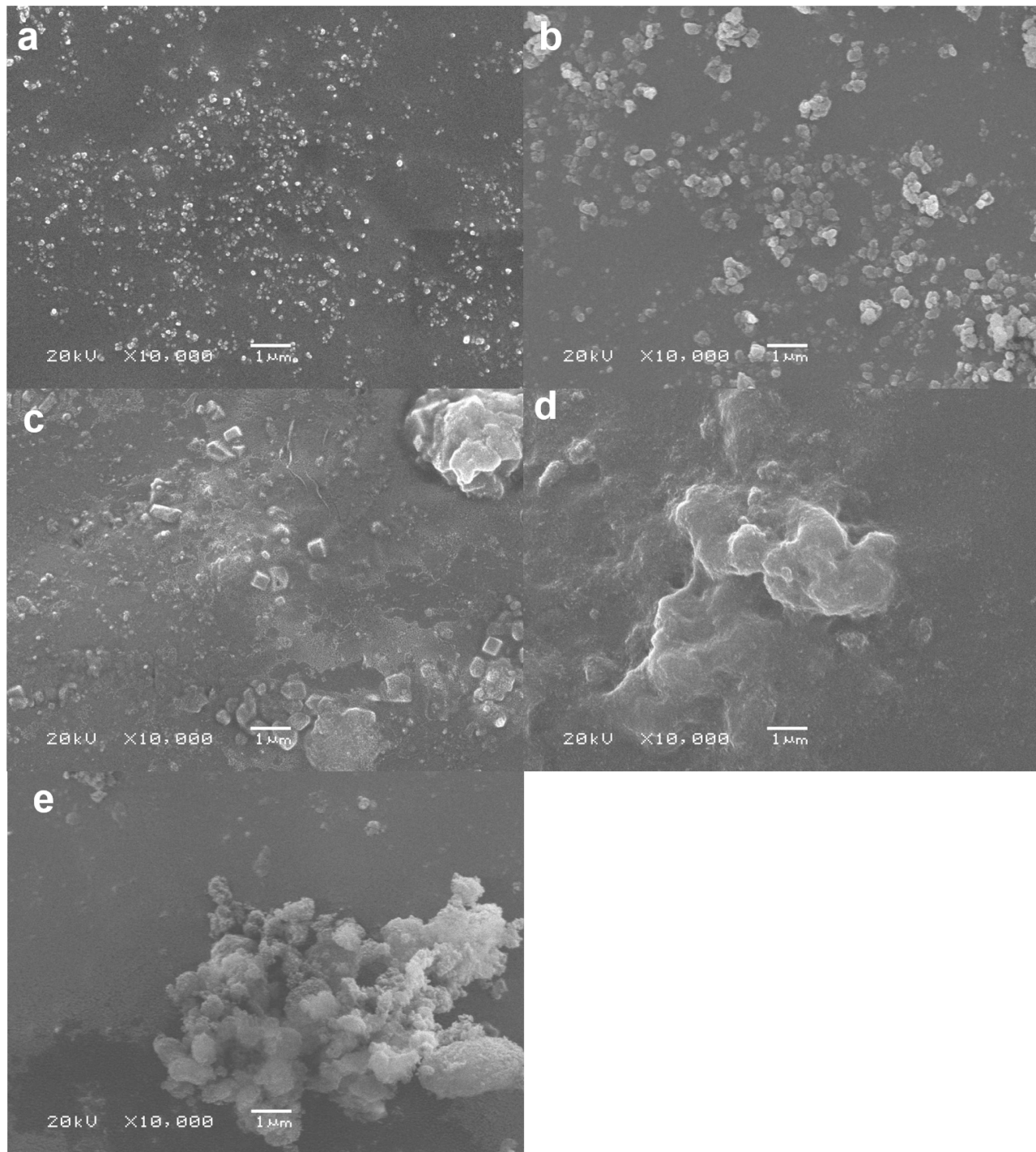


Figure 2. SEM images of powders hydrolysis at 20°C for 2 h with different addition of ammonia: (a) 0.5 mL, (b) 0.75 mL, (c) 1.0 mL, (d) 2.0 mL and (e) 3.0 mL.

Figure 2(a). In particular, the particle grows a little larger with uniform and well-dispersion at a point of 0.75 mL of ammonia content in **Figure 2(b)**, and the pH value is measured to be 8.5. Clearly, blocks are detected in **Figure 2(c)** to **Figure 2(e)**, indicating that severe agglomeration occurs in excess alkaline solutions. During the step of $\text{MgAl}_2(\text{OC}_3\text{H}_8)_8$ hydrolysis in an alkaline environment, the negatively charged Mg and Al nuclei appear by directly attacked by small anion OH^- radius, leading the cloud shift to the OR group on the other side. This further weakens the M-O bond and breaks out of the OR, and finally completes the hydrolysis reaction. With trace addition of ammonia, the rate of hydrolysis is relatively slow. At this point, it can be immediately spread widely to surroundings. That is, when the forming-speed of particles is smaller than that of the diffusion speed, the hydrolysis of $\text{MgAl}_2(\text{OC}_3\text{H}_8)_8$ acquires a very small particle size with a uniform particle size distribution. Continue to increase the amount of ammonia, the higher concentration of OH^- may enhance the hydrolysis rate and rate of colloidal particles. At that time, the agglomerates can be easily observed. Therefore, the controlling of pH in the hydrolysis process not only affects the gelation process but also plays a key role in the colloidal aggregation process. After all, the ideal hydrolysis pH is tuned to be 8.5 based on the formation in **Figure 2**.

The size distribution of samples with different addition of ammonia is listed in **Figure 3** and **Table 2**. As the increasing of ammonia, the particle size of the

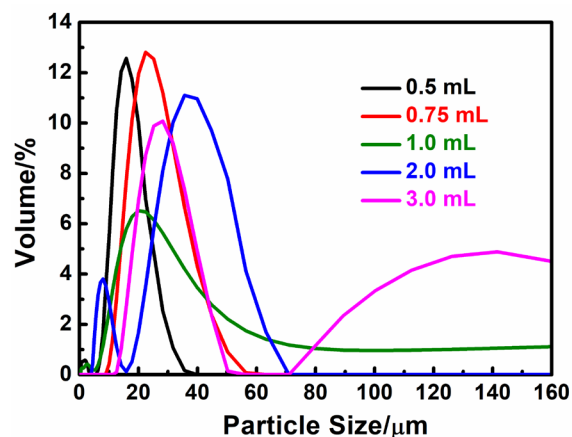


Figure 3. The size distribution of powders with different addition of ammonia from 0.5 mL to 3.0 mL.

Table 2. The particle size powders with different addition of ammonia in the range of 0.5 mL to 3.0 mL.

Ammonia (mL)	D10 (μm)	D50 (μm)	D90 (μm)
0.5	7.748	14.147	21.867
0.75	14.103	21.882	33.994
1.0	8.878	22.290	139.183
2.0	6.859	30.122	46.990
3.0	18.303	30.309	145.884

powder increases. With addition of 0.5 mL ammonia, it shows a main peak with the average particle size of 14.15 μm and a small peak around 2.0 μm , indicating that the higher proportion of small particles in the powder. When the amount of ammonia increases to 0.75 mL, there is a single peak with an average particle size of 21.88 μm . It further confirms that the particle size distribution is uniform with well agreement of SEM images in **Figure 2**. With continuously increased amount of ammonia, the particle size of the powder is gradually increased. When the amount of ammonia is 2.0 mL, the particle size is observed as two obvious distribution areas. There is no further no difference in the average particle size of the powder but the uniformity of particles deteriorates along with further excessive ammonia.

3.3. Effect of Dispersant during Hydrolysis

Dispersant, like CTAB and PVP, was selected to screen the particle distribution of samples. SEM images in **Figure S1** clearly exhibits that the spherical particle is obtained with the dispersant of CTAB, which is very different from that of sample with PVP. It further indicates that only certain dispersant of CTAB is benefit for creation the feature of particles. More importantly, we also compared the difference between the samples with or without CTAB dispersant for preparation of MgAl_2O_4 . The SEM image in **Figure 4(a)** exhibits that the agglomeration phenomenon is accessible without any dispersant. However, well-dispersion with spherical particles are obtained in **Figure 4(b)**. Based on the tendency described in **Figure 4(c)** and **Table 3**, the particle size of sample without any dispersant is centered to be about 43 μm and the distribution is unconcentrated. In contrast, the addition of CTAB greatly changes this phenomenon. The particle size decreases with the increase of CTAB content. Different amount of CTAB

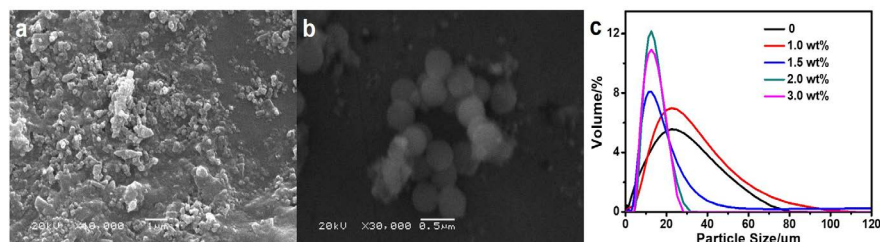


Figure 4. SEM images of MgAl_2O_4 : (a) without CTAB; (b) with 1.5 wt% CTAB and (c) the size distribution of samples with various amount of CTAB.

Table 3. The particle size of samples with different amount of CTAB.

Dispersant amount (wt%)	D10 (μm)	D50 (μm)	D90 (μm)
0	7.439	19.719	43.041
1.0	3.557	17.474	43.054
1.5	5.738	11.610	25.141
2.0	7.271	11.667	18.483
3.0	6.662	11.265	18.056

was screened from 0 to 3.0 wt% to further detect the particle size and its distribution in **Figure 4(c)**, indicating that the crucial factor of dispersant amount in the synthesis process. Especially for the point of 1.5 wt%, the particle size is greatly reduced and the distribution begins to concentrate. After that, the continuously increased amount of CTAB results in no more changes for particle size.

3.4. Effect of Alkoxide Concentration

SEM images in **Figure 5** illustrate the influenced concentration of $\text{MgAl}_2(\text{OC}_3\text{H}_8)_8$ on the morphology of hydroxides. The MgAl_2O_4 powder by introduction of 5 g alkoxide (**Figure 5(a)**) leads to a mixture of spherical particles and flocculent agglomerates. The average size of particles is determined to be about 400 nm. Some spherical particles are damaged and single spherical particle is found to aggregate with floc on the surface. Increasing the amount of alkoxide to 10 g in **Figure 5(b)**, it is found that spherical particles gradually decrease and agglomerate. The size distribution of floc aggregates is uneven and the boundary is irregular. With the addition of 15 g alkoxide in **Figure 5(c)**, spherical particles substantially disappear resulting in a white floc hydrolysate with a relatively uniform distribution with well dispersion, in which several opaque particles intersperse. It can be seen that alkoxide concentration has a great influence on the formation of colloids and particles during the hydrolysis reaction. It believes that it is mainly attributed to the extremely low concentration of alkoxide solution results in the restricted growth of nucleus to form sol. With increasing high concentration of alkoxide solution, the rapid formation of the nucleus under the state of supersaturation causes the crystal grains to have insufficient growth leading to small particle colloid. It is favorable for the growth of particles to form precipitates with moderate amount. In this work, it demonstrates that the sample with 10 g alkoxide possesses better morphology of spherical particles with well dispersion and uniform size distribution.

3.5. Effect of Hydrolysis Time

Figure 6 displays the SEM images of powders prepared with different hydrolysis time from 2 h to 72 h at 20°C. As shown in **Figure 6(a)**, numerous particles with

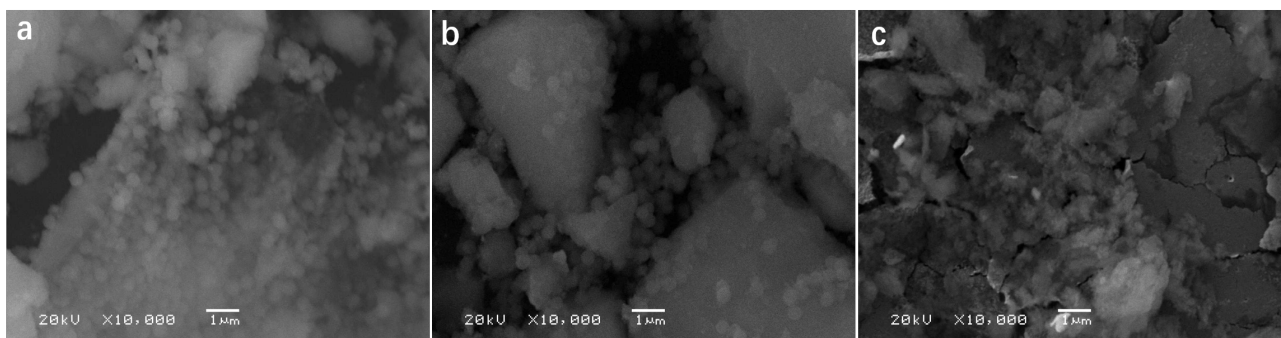


Figure 5. SEM images of $\text{MgAl}_2(\text{OH})_8$ with different amount of $\text{MgAl}_2(\text{OC}_3\text{H}_8)_8$: (a) 5 g, (b) 10 g and (c) 15 g. The hydrolysis reaction time is 24 h.

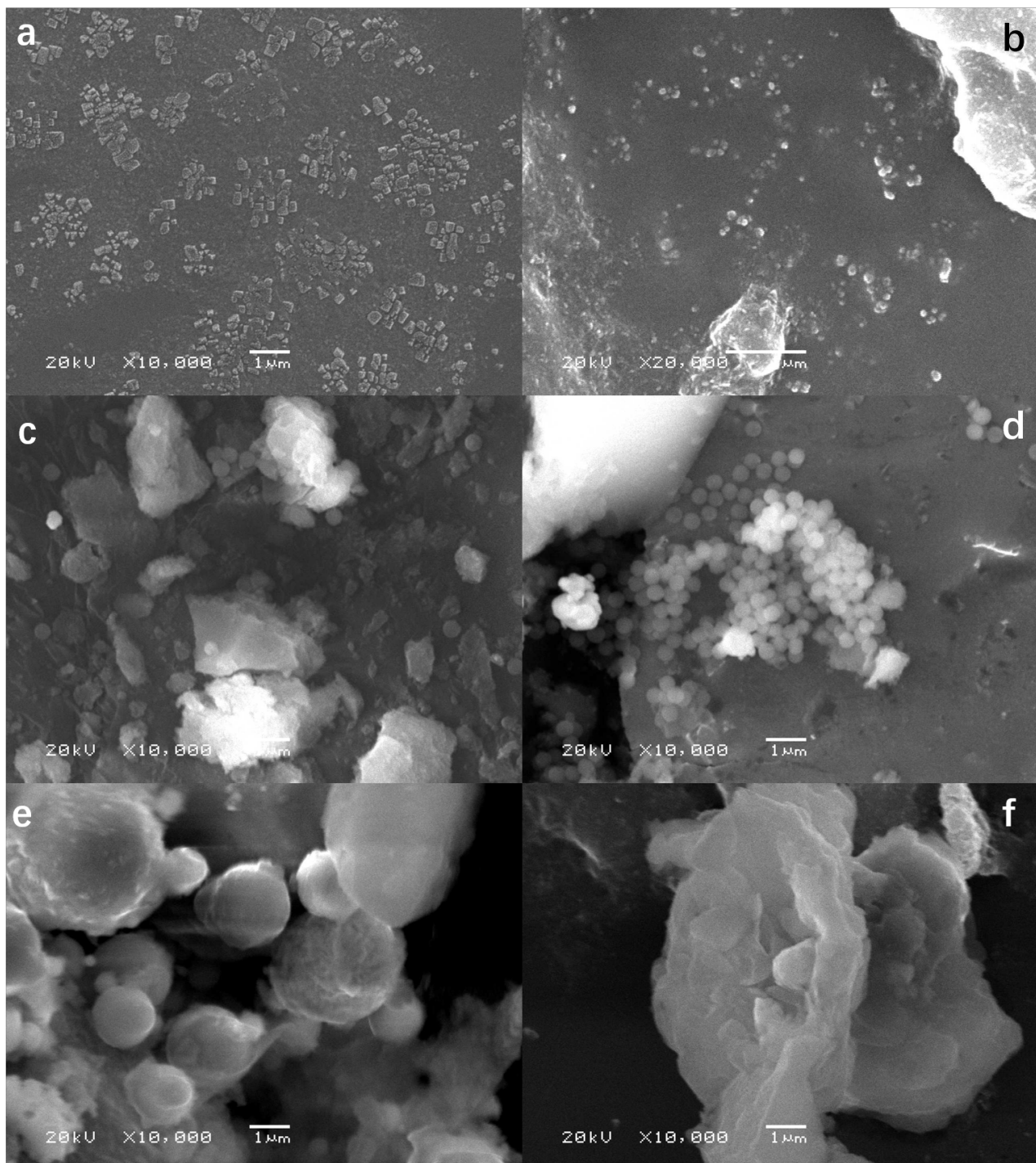


Figure 6. SEM images of $\text{MgAl}_2(\text{OH})_8$ prepared with different hydrolysis time: (a) 1 h; (b) 2 h; (c) 8 h; (d) 24 h; (e) 48 h and (f) 72 h.

angular, irregular shapes with a particle size of approximately 400 nm are observed under hydrolysis for 2 h. Particles gradually grow to flocculated agglomerates under hydrolysis for 2 h in **Figure 6(b)**. Extend the hydrolysis time directly to 8 h in **Figure 6(c)**, it is found that most hydrolysate is detected to be agglomerates with various particle sizes and irregular shapes. But it still can be

observed that a small amount of spherical or near-spherical particles are attached to the agglomerates. Along with the hydrolysis time for 24 h in **Figure 6(d)**, the as-prepared spherical particles gradually increase with uniform particle size of 300 to 400 nm and well-distribution, meanwhile, the agglomerates are gradually reduced. Continue to extend the reaction time to 48 h in **Figure 6(e)**, spherical particles are found to gradually reduce with larger size and the irregularly agglomerates increase. Here, agglomeration occurs between particles and agglomerates. Until to 72 h the spherical particles disappeared, and all the substances obtained are flocculent agglomerates in **Figure 6(f)**.

3.6. Effect of Hydrolysis Temperature

The hydrolysis temperature is considered to be another important factor that may influence the property of magnesium aluminum spinels. **Table 4** and **Figure 7** show the particle size, surface area and size distribution of samples hydrolysis at various temperatures from 20°C to 60°C. The crystal growth rate and particle size greatly increase as the increasing hydrolysis temperature below 40°C. The higher temperature results in the wider the particle size distribution. Analysis demonstrates that such phenomenon is caused by hydrolysis temperature, particularly at 50°C and 60°C. Such high hydrolysis temperature causes

Table 4. The particle size and surface area of samples at different hydrolysis temperature from 20°C to 60°C.

Temperature (°C)	D10 (μm)	D50 (μm)	D90 (μm)	Surface area (m ² /g)
20	3.729	10.362	19.874	6.44
30	6.662	11.265	18.056	5.82
40	8.034	17.020	31.283	6.74
50	7.725	17.697	51.686	4.44
60	1.019	16.538	84.880	5.65

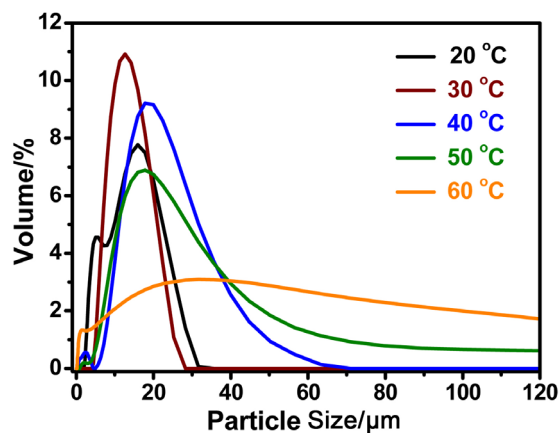


Figure 7. The particle size distribution of the samples with isopropanol as precursor solvent at hydrolysis temperature from 20°C to 60°C.

rapid formation of numerous crystals and later larger crystals become to generate. As a consequence, the optimal hydrolysis temperature is acquired to be 40°C.

3.7. Effect on Calcination Temperature

Thermogravimetry and differential thermogravimetry (TG-DTG) curves were conducted on obtained powders with different types of alkoxides from 50°C to 900°C in **Figure 8**. In **Figure 8(a)**, there are two stages for sample with ethanol as precursor with a total mass loss of 35% during the whole warming interval. During the lower temperature from 50°C to 200°C, the weight loss is about 20% due to physical adsorption of water as well as residual solvent residues in the reaction. The weight loss of 15% is ascribed in the range of 200°C to 600°C as desorption of dihydroxylation from ethanol and chemical bond break between a trace amount of ethyl and magnesium or aluminum ions. After that, it turned to be stable without any weight loss. As shown in **Figure 8(b)** and **Figure 8(c)**, there are three stages for samples with n-butanol and isopropanol as precursors

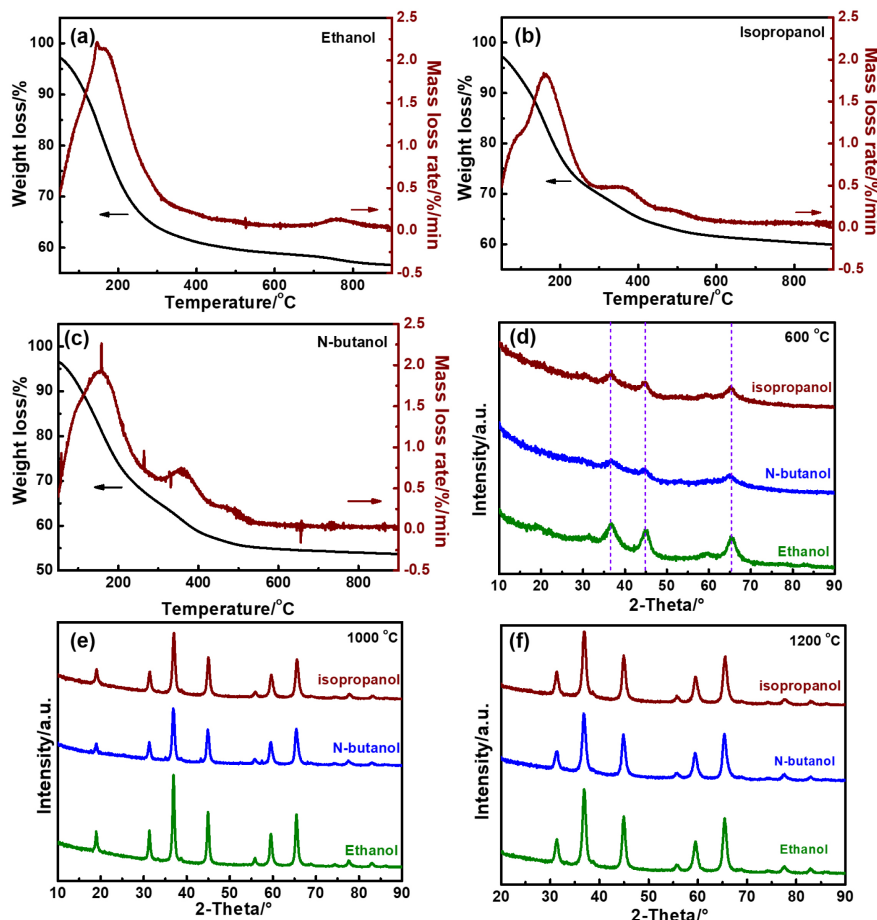


Figure 8. The TG-DTG curves of samples with different organic alcohols of (a) ethanol, (b) isopropanol and (c) n-butanol and (d) particle size distribution of corresponding samples with various magnesium aluminum bimetal alkoxide after dried 80°C and further hydrolysis; XRD patterns (e), (f) and (g) of samples with different organic alcohols treated at various temperature (600°C, 1000°C and 1200°C).

with total mass loss of 45% and 38%, respectively. As for the first stage, the weight loss of 18% and 16% for $\text{MgAl}_2(\text{OH})_8$ prepared with n-butanol and isopropanol from 50°C to 200°C can be ascribed as physical adsorption of water as well as residual solvent residues in the reaction. For the second step, the weight loss of 20% and 18% for $\text{MgAl}_2(\text{OH})_8$ with n-butanol and isopropanol during 200°C to 400°C are due to dehydroxylation from the precursors. In the third period, slightly mass loss happens of 7% and 4% for samples with n-butanol and isopropanol from 400°C to 600°C, which may be caused by a chemical bond break between a trace amount of residual butyl or isopropyl group and magnesium or aluminum ions. After that, no more weight loss occurs. An endothermic peak of precursor with n-butanol is significantly larger than that of sample with isopropanol, indicating that preparation of sample with n-butanol needs more energy than that with isopropanol. Besides, both of precursors with n-butanol and isopropanol need more energy than that of ethanol. Additionally, the structure of obtained powders with various precursors of alkoxides was detected by XRD in **Figure 8** and **Table 5**. As shown in **Figures 8(d)-(f)**, XRD was conducted on samples prepared with various precursors of alkoxides and calcinated at a wide range temperature of 600°C, 1000°C and 1200°C for 3 h. The result of XRD patterns clearly indicates that powders with various alkoxides are consistent well with pure magnesium aluminum spinel structure without too much change in the position of the diffraction peak. The lattice intensity enhances with the increasing temperature from 600°C to 1200°C, indicating that the degree of crystallization of spinel increases with the increasing calcinated temperature. Based on the data in **Figure 8(e)**, the intensity of diffraction peaks of sample with ethanol as alkoxide is significantly higher than that of n-butanol and isopropanol. It demonstrates that the required temperature for spinel phase with ethanol is low, which is consistent well with the data in **Figure 8**. On the other hand, the relative intensities of the diffraction peaks of each sample become smaller with the increasing temperature. Each sample displays the same relative intensities at 1200°C in **Figure 8(f)**. Considering avoiding the severe aggregation of large particles at too much higher temperature, thus the optimal calcination temperature is selected to be 1200°C.

As shown in **Table 5**, there is an obvious change of particle size among powders with ethanol, isopropanol and n-butanol as organic alcohol solvent in precursor preparation. The D50 of size distribution are 14.15 µm, 17.70 µm and 24.83 µm for sample with ethanol, isopropanol and n-butanol in **Table 5**, indicating that

Table 5. The particle size of samples with various alkoxides after treated at 1200°C.

Types of alkoxides	D10 (µm)	D50 (µm)	D90 (µm)	Surface area (m ² /g)
Ethanol	7.981	14.146	28.045	4.51
Isopropanol	7.725	17.697	51.686	4.82
N-butanol	9.159	24.829	61.373	3.80

the particle size of powders increases with the increasing carbon chain of organic alcohol. Among them, the average particle size of the corresponding powder of n-butanol is the smallest. Based on the analysis of particle size distribution, the particle size of isopropanol is relatively concentrated with largest specific surface area. As a result, MgAl_2O_4 with isopropanol as solvent for synthesis of precursor was better than that of ethanol and n-butanol in terms of particle size and corresponding distribution.

4. Conclusion

All in all, various synthetic parameters were deeply investigated on the preparation of MgAl_2O_4 via sol-gel followed by high temperature pyrolysis. The optimal preparation factors are as follows: 1) The alkoxide prepared with isopropanol possesses a larger surface area with uniform particle size; 2) Addition of ammonia with a pH of 8.5 can enhance the hydrolysis rate and rate of colloidal particles; 3) The point addition of 1.5 wt% of CTAB results in greatly reduced particle size with concentrated distribution of particles; 4) The moderate amount of alkoxide (10 g) with hydrolysis at 40°C for 24 h shows uniform particle and well-distribution; 5) the optimal calcination temperature of 1200°C introduces a pure magnesium aluminum spinel.

Acknowledgements

This work was partially supported by National Natural Science Fund of China (Grant Nos. 21606219).

Conflicts of Interest

The authors declare no conflict of interest.

References

- [1] Rubat du Merac, M., Kleebe, H.J., Müller, M.M. and Reimanis, I.E. (2013) Fifty Years of Research and Development Coming to Fruition; Unraveling the Complex Interactions during Processing of Transparent Magnesium Aluminate (MgAl_2O_4) Spinel. *Journal of the American Ceramic Society*, **96**, 3341-3365.
<https://doi.org/10.1111/jace.12637>
- [2] Hadian, N., Rezaei, M., Mosayebi, Z. and Meshkani, F. (2012) CO₂ Reforming of Methane over Nickel Catalysts Supported on Nanocrystalline MgAl_2O_4 with High Surface Area. *Journal of Natural Gas Chemistry*, **21**, 200-206.
[https://doi.org/10.1016/S1003-9953\(11\)60355-1](https://doi.org/10.1016/S1003-9953(11)60355-1)
- [3] Mosayebi, Z., Rezaei, M., Ravandi, A.B. and Hadian, N. (2012) Autothermal Reforming of Methane over Nickel Catalysts Supported on Nanocrystalline MgAl_2O_4 with High Surface Area. *International Journal of Hydrogen Energy*, **37**, 1236-1242.
<https://doi.org/10.1016/j.ijhydene.2011.09.141>
- [4] Zhu, L.L., Park, Y.-J., Gan, L., Go, S.-I., Kim, H.-N., Kim, J.-M. and Ko, J.-W. (2018) Fabrication of Transparent MgAl_2O_4 from Commercial Nanopowders by Hot-Pressing without Sintering Additive. *Materials Letters*, **219**, 8-11.
<https://doi.org/10.1016/j.matlet.2018.02.010>

- [5] Xu, W.W. and Dávila, L.P. (2018) Effects of Crystal Orientation and Diameter on the Mechanical Properties of Single-Crystal MgAl₂O₄ Spinel Nanowires. *Nanotechnology*, **30**, Article ID: 055701.
<https://iopscience.iop.org/article/10.1088/1361-6528/aaef11/meta>
<https://doi.org/10.1088/1361-6528/aaef11>
- [6] Malekabadi, M.A. and Mamoory, R.S. (2018) Low-Temperature Synthesis of Micro/Nano Lithium Fluoride Added Magnesium Aluminate Spinel. *Ceramics International*, **44**, 20122-20131. <https://doi.org/10.1016/j.ceramint.2018.07.305>
- [7] Ding, D.H., Lv, L.H., Xiao, G.Q., Ren, Y., Yang, S.L., Yang, P. and Hou, X. (2019) One-Step Synthesis of *in Situ* Multilayer Graphene Containing MgAl₂O₄ Spinel Composite Powders. *Ceramics International*, **45**, 6209-6215.
<https://doi.org/10.1016/j.ceramint.2018.12.098>
- [8] Schneider, D., Mehlhorn, D., Zeigermann, P., Kärger, J. and Valiullin, R. (2016) Transport Properties of Hierarchical Micro-Mesoporous Materials. *Chemical Society Reviews*, **45**, 3439-3467.
<https://pubs.rsc.org/en/content/articlehtml/2016/cs/c5cs00715a>
<https://doi.org/10.1039/C5CS00715A>
- [9] DeCanio, E.C. and Weissman, J.G. (1995) FT-IR Analysis of Borate-Promoted Ni-Mo/Al₂O₃ Hydrotreating Catalysts. *Colloids and Surfaces A: Physicochemical and Engineering Aspects*, **105**, 123-132.
[https://doi.org/10.1016/0927-7757\(95\)03307-3](https://doi.org/10.1016/0927-7757(95)03307-3)
- [10] Habibi, N., Wang, Y., Arandian, H. and Rezaei, M. (2017) Low-Temperature Synthesis of Mesoporous Nanocrystalline Magnesium Aluminate (MgAl₂O₄) Spinel with High Surface Area Using a Novel Modified Sol-Gel Method. *Advanced Powder Technology*, **28**, 1249-1257. <https://doi.org/10.1016/j.apt.2017.02.012>
- [11] Areán, C.O., Mentruit, M.P., López, A.L. and Parra, J. (2001) High Surface Area Nickel Aluminate Spinels Prepared by a Sol-Gel Method. *Colloids and Surfaces A: Physicochemical and Engineering Aspects*, **180**, 253-258.
[https://doi.org/10.1016/S0927-7757\(00\)00590-2](https://doi.org/10.1016/S0927-7757(00)00590-2)
- [12] Liu, W., Yang, J.L., Xu, H., Wang, Y.Z., Hu, S.L. and Xue, C.Y. (2013) Effects of Chelation Reactions between Metal Alkoxide and Acetylacetone on the Preparation of MgAl₂O₄ Powders by Sol-Gel Process. *Advanced Powder Technology*, **24**, 436-440. <https://doi.org/10.1016/j.apt.2012.09.006>
- [13] Parmentier, J., Richard-Plouet, M. and Vilminot, S. (1998) Influence of the Sol-Gel Synthesis on the Formation of Spinel MgAl₂O₄. *Materials Research Bulletin*, **33**, 1717-1724. [https://doi.org/10.1016/S0025-5408\(98\)00169-X](https://doi.org/10.1016/S0025-5408(98)00169-X)
- [14] Suyama, Y. and Kato, A. (1982) Characterization and Sintering of Mg-Al Spinel Prepared by Spray-Pyrolysis Technique. *Ceramics International*, **8**, 17-21.
[https://doi.org/10.1016/0272-8842\(82\)90010-4](https://doi.org/10.1016/0272-8842(82)90010-4)
- [15] Rashad, M., Zaki, Z. and El-Shall, H. (2009) A Novel Approach for Synthesis of Nanocrystalline MgAl₂O₄ Powders by Co-Precipitation Method. *Journal of Materials Science*, **44**, 2992-2998.
<https://link.springer.com/article/10.1007/s10853-009-3397-8>
<https://doi.org/10.1007/s10853-009-3397-8>
- [16] Navaei Alvar, E., Rezaei, M., Navaei Alvar, H., Feyzallahzadeh, H. and Yan, Z.-F. (2009) Synthesis of Nanocrystalline MgAl₂O₄ Spinel by Using Ethylene Diamine as Precipitation Agent. *Chemical Engineering Communications*, **196**, 1417-1424.
<https://doi.org/10.1080/00986440902939012>
- [17] Amini, M., Mirzaee, M. and Sepanj, N. (2007) The Effect of Solution Chemistry on

the Preparation of MgAl_2O_4 by Hydrothermal-Assisted Sol-Gel Processing. *Materials Research Bulletin*, **42**, 563-570.

<https://doi.org/10.1016/j.materresbull.2006.06.011>

- [18] Balabanov, S., Vaganov, V., Gavrilchuk, E., Drobotenko, V., Permin, D. and Fedin, A. (2014) Effect of Magnesium Aluminum Isopropoxide Hydrolysis Conditions on the Properties of Magnesium Aluminate Spinel Powders. *Inorganic Materials*, **50**, 830-836. <https://link.springer.com/article/10.1134/S0020168514080032>
<https://doi.org/10.1134/S0020168514080032>

Supplement

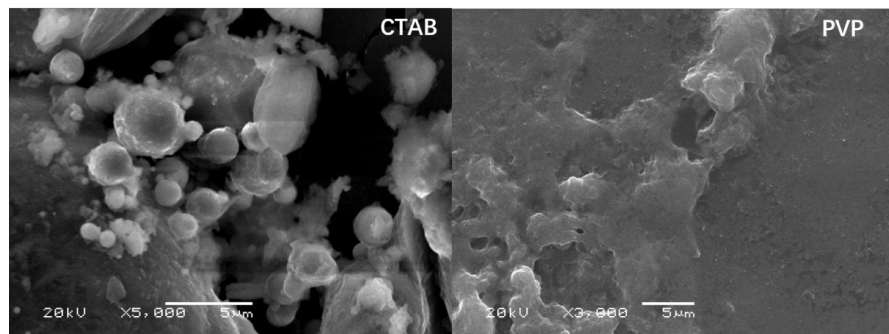


Figure S1. SEM images of $\text{MgAl}_2(\text{OC}_3\text{H}_8)_8$ with dispersant of (a) CTAB and (b) PVP.